Synthesis and Thermal Properties of Polythioetherimides Derived from 4,4'-[p-Thiobis(phenylenesulfanyl)]Diphthalic Anhydride and Various Aromatic Diamines

JIN-GANG LIU[1,2]
Laboratory of Advanced Polymer Materials, Institute of Chemistry, Chinese Academy of Sciences, Beijing 100080, People's Republic of China

YUJI SHIBASAKI
SHINJI ANDO
MITSURU UEDA
Department of Organic and Polymeric Materials, Tokyo Institute of Technology, 2-12-1-H120, O-okayama, Meguro-ku, Tokyo 152-8552, Japan

(Received 26 May 2007; accepted 5 July 2007)

Abstract: An asymmetrical aromatic diamine, 1-(4'-aminophenoxy)-4-(4'-aminophenylenesulfanyl) benzene (OSDA) was synthesized. A series of polythioetherimides (PTEIs) were prepared from a thioether-bridged aromatic dianhydride 4,4'-[*p*-thiobis(phenylenesulfanyl)]diphthalic anhydride (3SDEA) and various aromatic diamines having ether or thioether linkages between phenylene rings by a two-step polycondensation procedure via their soluble poly(amic acid) (PAA) precursors. Medium to high molecular weight PAAs were obtained with inherent viscosities near or higher than 1.0 dL g^{-1}, which is high enough to afford flexible and tough PTEI films except for PI-2 (3SDEA-134APB) and PI-6 (3SDEA-*m*2SPDA) derived from *meta*-ether-substituted diamines. PI-2 and PI-6 showed some extent of crystallinity compared to the amorphous natures of the other polymers. The PTEI films exhibit good resistance to organic solvents except for PI-3 (3SDEA-133APB), which is soluble in *N*-methyl-2-pyrrolidinone (NMP) and sulfuric acid at room temperature. The PTEI films show good thermal stability with the 5% weight loss temperatures being above 480°C both in nitrogen and in air. The glass transition temperatures of the PTEIs are in the range of 155–191°C, which are lower than those of the commercial polyetherimides due to their plural thioether linkages in the main chains.

Key Words: Polythioetherimide, thermal stability, thioether, high refractive index

High Performance Polymers, **20:** 221–237, 2008 DOI:10.1177/0954008307082508

1. INTRODUCTION

Polyetherimide (PEI) and poly(phenylene sulfide) (PPS) are two classes of important high performance engineering polymers, characterized by their high service temperature, easy processability, high mechanical and dielectric properties and inherent flame retardancy [1–3]. The excellent combined properties of these two polymers come from their special structural characteristics. For example, the flexible oxygen-ether linkages in PEI and thioether moieties in PPS endow them with special properties, such as the eximious processability for PEI and the excellent chemical resistance and good adhesion for PPS [4–6]. However, in practice, the low impact strength and low glass transition temperatures of PPS [7] and the unsatisfactory solvent resistance and poor adhesion for PEI often limit their wide applications. Thus, it would be a significant endeavor to combine the good properties of these two polymers, namely to develop novel polythioetherimides (PTEIs).

In the literature, to our knowledge, some pioneering works have been performed on PTEIs, such as the PTEIs based on 3,3',4,4'-thiodiphenyltetracarboxylic dianhydride [8], those based on diamine-terminated oligo(phenylene thioether)s [9], and those derived from chloro-displacement polymerization of substituted phthalimides and thiolates [10]. The applications include high temperature adhesives for bonding steels [11], high temperature composites [12] and gas separation membranes [13]. Recently, the research and development of PTEIs have been motivated by the increasing demands of polymers with high refractive indices for advanced optical applications [14]. In our laboratory, a series of PTEIs have been developed, which exhibited good thermal stability and refractive indices as high as 1.76 [15–17].

With the aim of developing high performance sulfur-containing polymers, the effects of structural varieties on the thermal properties of PTEIs, including thermal and thermal-oxidative stability, glass transition, melt crystallization and thermal degradation were systemically studied in this work. For this purpose, an aromatic dianhydride containing three thioether linkages in the molecular repeating unit 3SDEA was synthesized according to our previous work. An asymmetrical aromatic diamine, 1-(4'-aminophenoxy)-4-(4'-aminophenylenesulfanyl) benzene (OSDA) was newly synthesized and several commercially-available ether-linked diamines were also utilized for the polymerizations.

2. EXPERIMENTAL

2.1. Materials

p-Hydroxythiophenol, *p*-chloronitrobenzene, 4-bromophthalic anhydride, 4,4'-thiobisbenzenethiol, 1,4-bis(4-aminophenoxy)benzene (144APB), 1,3-bis(4-aminophenoxy) benzene (134APB), and 1,3-bis(3-aminophenoxy)benzene (133APB) were purchased from TCI, Japan, and used as received. 4,4'-[*p*-Thiobis(phenylenesulfanyl)]diphthalic anhydride (3SDEA) [16], 4,4'-(*p*-phenylenedisulfanyl)dianiline (2SPDA) [15] and 4,4'-

(*m*-phenylenedisulfanyl)dianiline (*m*2SPDA) [15] were synthesized according to our previous work. Palladium on activated carbon (10%), hydrazine monohydrate, 2-methoxyethanol, anhydrous *N*-methyl-2-pyrrolidinone (NMP), *N,N*-dimethlformamide (DMF) and anhydrous potassium carbonate were obtained from Wako, Japan and used as received.

2.2. Measurements

^{1}H and ^{13}C spectra were recorded on a Varian Mercury 300 spectrometer using $CDCl_3$ or DMSO-d_6 as solvent and tetramethylsilane (TMS) as reference. Inherent viscosity was measured using an Ubbelohde-viscometer with a 0.5 g dL^{-1} NMP solution at 30°C. Fourier transform infrared (FT IR) spectra were obtained with a Horiba FT-120 Fourier transform spectrophotometer. Ultraviolet-visible (UV Vis) spectra were recorded on a Hitachi U-3210 spectrophotometer at room temperature. PI films were dried at 100°C for 1 h before testing to remove the absorbed moisture. The wide-angle X-ray diffraction (XRD) was conducted on a Rigaku D/max-2500 X-ray diffractometer with Cu/K-α1 radiation, operated at 40 kV and 200 mA. Thermogravimetric analysis (TGA) was recorded on a Seiko TG/DTA 6300 thermal analysis system at a heating rate of 10°C min^{-1} in flow nitrogen or in air (200 mL min^{-1}). Differential scanning calorimetry (DSC) was performed on a Seiko DSC 6300 at a heating rate of 10°C min^{-1} in nitrogen (200 mL min^{-1}). Dynamic mechanical thermal analysis (DMA) was performed on PTEI film specimens (30 mm long, 10 mm wide, and 50–60 μm thick) on a Seiko DMS 6300 at a heating rate of 2°C min^{-1} with a load frequency of 1 Hz in air. The glass transition temperature (T_g) is determined as the peak temperature of loss modulus (E'') plot. Solubility of the PTEI films was evaluated as follows. PI film specimen (0.1 g) was mixed with a specific solvent (9.9 g) at room temperature and then stirred for 24 h. Solubility was determined visually as three grades: completely soluble (++), partially soluble (+–) and insoluble (–).

The optical absorptions of the PTEI films in the UV-visible region are predicted by using the time-dependent density functional theory (TD-DFT) [15].

2.3. Monomer synthesis

2.3.1. Synthesis of 1-(4'-nitrophenoxy)-4-(4'-nitrophenylenesulfanyl)benzene (OSDN).

A mixture of *p*-chloronitrobenzene (34.66 g, 0.22 mol), *p*-hydroxythiophenol (12.62 g, 0.10 mol), anhydrous K_2CO_3 (31.79 g, 0.23 mol) and freshly-distilled *N,N*-dimethylformamide (200 mL) was added to a three-necked 250-mL flask equipped with a magnetic stirrer, a nitrogen inlet and a condenser. The mixture was heated to reflux in nitrogen for 24 h. The solvent was removed by vacuum distillation. The mixture was poured into an excess amount of water. The precipitate was collected by filtration, washed with water and dried in vacuo at 100°C for 24 h. The obtained yellow powder was recrystallized from 2-methoxyethanol to afford pale yellow crystals (OSDN) with yield: 25.2 g (68.3%), mp: 200.9°C (DSC peak temperature). FT IR (KBr, cm^{-1}): 1577.5, 1508.1, 1484.9, 1334.5, 1238.1, 1164.8, 1110.8, 875.5, and 840.8. ^{1}H NMR (300 MHz, DMSO-d_6, ppm): 7.15–

7.25 (m, 6H), 7.57–7.59 (d, 2H), 8.02–8.05 (d, 2H), and 8.17–8.19 (d, 2H). Elemental analysis: Calculated for $C_{18}H_{12}N_2O_5S$: C, 58.69%; H, 3.28%; N, 7.60%. Found: C, 58.54%; H, 3.37%; N, 7.57%.

2.3.2. Synthesis of 1-(4'-aminophenoxy)-4-(4'-aminophenylenesulfanyl)benzene (OSDA).

A mixture of OSDN (15.92 g, 0.043 mol), absolute ethanol (180 mL) and a catalytic amount of 10% palladium on activated carbon (1.2 g) was added a 250-mL three-necked flask fitted with a magnetic stirrer, a thermometer and a dropping funnel. The reaction mixture was heated to reflux and then hydrazine monohydrate (90 mL) was added dropwise over a period of 1.5 h. After the addition was completed, the reaction system was refluxed for 24 h. The mixture was then filtered hot to remove the catalyst and the filtrate was cooled to room temperature. Deionized water (100 mL) was added, and the precipitated white needle crystals were filtered out, washed with cold ethanol and dried under vacuo at 80°C overnight to afford OSDA. The diamine was purified by recrystallization from ethanol-water mixture (7:3, v/v) as white crystals. Yield: 10.58 g (79.4%); mp: 126.8°C (DSC peak temperature). FT IR (KBr, cm^{-1}): 3409.5, 3320.8, 1631.5, 1596.8, 1484.9, 1288.2, 1230.4, 1172.5, and 821.5. ^{1}H NMR (300 MHz, DMSO-d_6, ppm): 4.87(s, 2H), 5.31 (s, 2H), 6.56–6.58 (d, 4H), 6.70–6.79 (m, 4H), and 7.05–7.13 (m, 4H). ^{13}C NMR (300MHz, DMSO-d_6, ppm): 158.2, 150.4, 146.4, 136.2, 132.3, 130.3, 121.6, 118.1, 117.8, 115.8, and 115.6. Elemental analysis: calculated for $C_{18}H_{16}N_2OS$: C, 70.10%; H, 5.23%; N, 9.08%. Found: C, 69.96%; H, 5.41%; N, 9.02%.

2.3.3. Polyimide synthesis

A typical preparation of the PTEIs proceeds as follows. To a well-dried 50-mL three-necked flask equipped with a nitrogen inlet and an electromagnetic stirrer was added OSDA (1.5420 g, 5 mmol) and anhydrous NMP (15.0 g). The mixture was stirred with a cold water bath to afford a clear diamine solution. 3SDEA (2.7130 g, 5 mmol) was added incrementally to the diamine solution within 30 min. Additional NMP (2.0 g) was added to adjust the solid content of the mixture to be 20 wt%. The cold water bath was removed and the reaction mixture was stirred at room temperature for 24 h to give a viscous solution, yellow in color. The obtained PAA-4 solution was diluted (10 wt%) and filtered through a 0.45 μm Teflon syringe filter and cast onto a silicon wafer. The thickness of the film was controlled by spin-coating rate. For example, the thickness of a specimen for FT IR and UV Vis measurement was controlled to be about 10 μm, and the specimen for thermal property evaluation was adjusted to be about 50 μm. PI-4 film was obtained by thermally curing the PAA-4 film in an oven for 1 h at each of 80°C, 150°C, 250°C, 300°C, respectively. The PI films were peeled by immersing the Si wafer in warm water.

The other films, including PI-1 (3SDEA-144APB), PI-2 (3SDEA-134APB), PI-3 (3SDEA-133APB) and PI-6 (3SDEA-*m*2SPDA) were prepared according to the similar procedure as mentioned above. PI-5 (3SDEA-2SPDA) was prepared according to our previous work [15].

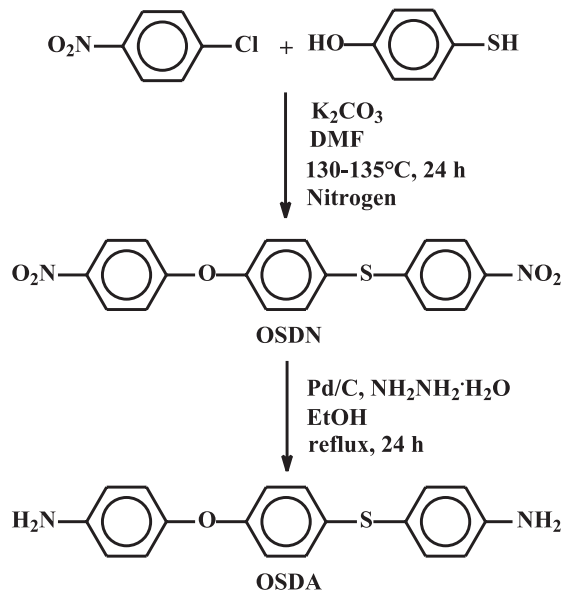

Scheme 1. Synthesis of OSDA.

3. RESULTS AND DICUSSION

3.1. Monomer synthesis

An asymmetrical aromatic diamine OSDA was synthesized by the well-established nucleophilic displacement reaction of *p*-chloronitrobenzene and *p*-hydroxythiophenol, as shown in scheme 1. The structure of the diamine was confirmed by FT IR (figure 1) and NMR (figure 2). In the FT IR spectra, the characteristic absorptions of nitro group located at 1577 cm^{-1} and 1338 cm^{-1} in OSDN disappear in the spectrum of OSDA, whereas the typical absorptions of amino group at 3409 cm^{-1} and 3320 cm^{-1} are obviously observed. In the ^{1}H NMR spectrum, the two amino protons (amino ① and amino ②) exhibit different chemical shift values due to the different chemical circumstances. Amino ① located at the *para*-position of oxygen-ether linkage has a lower chemical shift value compared to that of amino ② due to the higher electron-donating ability of oxygen-ether than that of thioether group. In the ^{13}C NMR spectrum, twelve signals are observed, which is consistent with the chemical structure and symmetry of the diamine.

3.2. Polyimide synthesis and film properties

The most frequently utilized methods for the preparation of PTEIs include the two-step low temperature and one-step high temperature polycondensations of sulfur-containing

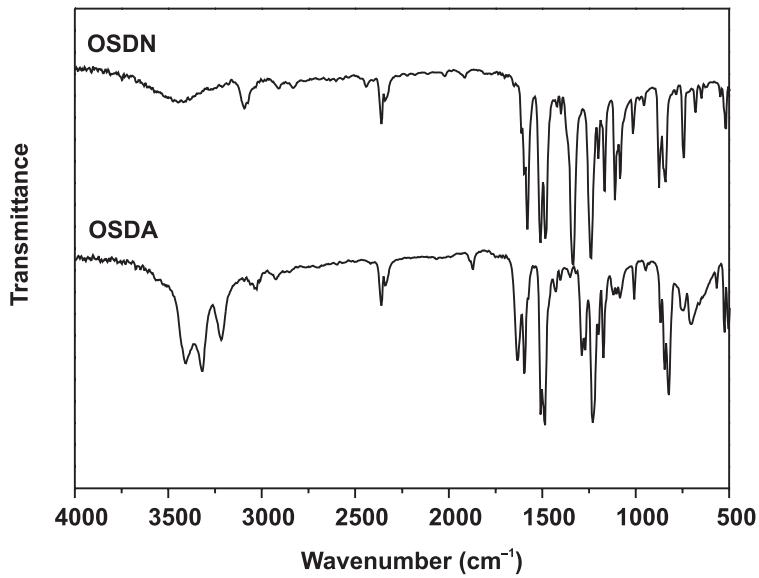

Figure 1. FT IR spectra of OSDN and OSDA (KBr flake).

Table 1. Polymerization and film properties of PTEIs.

PI	Diamine	$[\eta]_{inh}$ [a]	Film [b]		Solubility [c]			
		(dL g^{-1})	~10 μm	~50 μm	NMP	*m*-cresol	H_2SO_4	ME
PI-1	144APB	1.13	F.T.	F.T.	–	–	+–	–
PI-2	134APB	1.11	F.T.	B.O.	–	–	+–	–
PI-3	133APB	0.95	F.T.	F.T.	++	+–	+–	–
PI-4	OSDA	1.26	F.T.	F.T.	–	–	+–	–
PI-5	2SPDA	0.66	F.T.	F.T.	–	–	+–	–
PI-6	*m*2SPDA	0.98	F.O.	B.O.	–	–	+–	–

[a] Measured with PAA solution at a concentration of 0.5 g dL^{-1} at 30°C.
[b] F: flexible; B: brittle; T: transparent; O: opaque.
[c] Measured at a polymer concentration of 1% (w/w). ++: soluble; +–: partially soluble; –: insoluble; ME: 2-methoxyethanol.

diamines or dianhydrides. In the present work, the PTEIs were synthesized from the ether diamines listed in table 1 and 3SDEA via a two-step procedure, according to scheme 2. The poly(amic acid) (PAA) precursors had inherent viscosities of 0.66–1.13 dL g^{-1}, indicating the high molecular weights and good purity of the monomers. Two kinds of films – thin films for IR and UV measurements and thick films for thermal evaluations – were prepared from the PAA solutions. The characteristic absorptions of imide moieties, i.e.

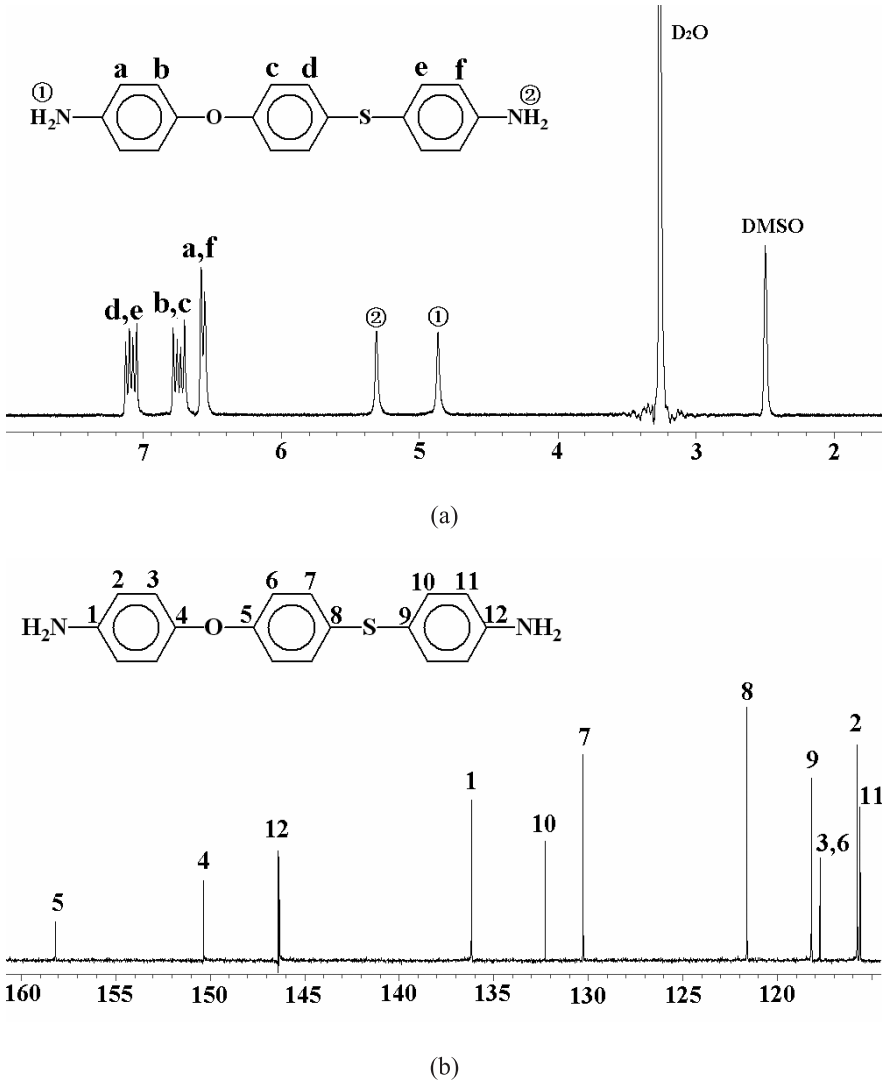

Figure 2. ^{1}H (a) and ^{13}C NMR (b) spectra of OSDA (DMSO-d_6, 300MHz).

~1780 cm^{-1} ($\upsilon_{C=O,as}$) and ~1720 cm^{-1} ($\upsilon_{C=O,s}$) for carbonyl, and ~1385 cm^{-1} for C-N bond indicate the successful preparation of the PTEIs.

All the films show flexible, tough and transparent natures except for thick PI-2 and PI-6 films, which are brittle and opaque. This phenomenon might be explained by the semi-crystalline structures of these two polymers, which will be discussed below. The crystallinity of PI-2 can also be confirmed by the WAXD X-ray diffraction patterns,

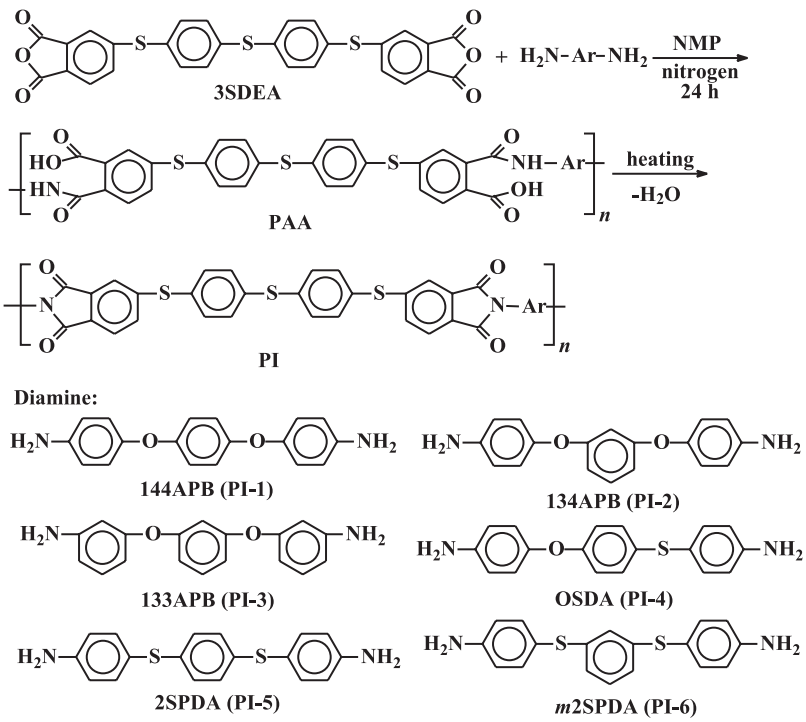

Scheme 2. Synthesis of PTEIs.

as shown in figure 3. The PTEIs derived from *para*-substituted diamines (PI-1 and PI-4) and whole-*meta*-substituted diamine (PI-3) show typical amorphous natures.

The experimental and predicated optical transparency of the PTEI films was illustrated in figure 4. Similar curves were obtained with the cutoff-wavelengths at ~400 nm and at transmittances of higher than 80% at 450 nm. The experimental spectra are well reproduced by the calculated spectra, which demonstrate that thioether linkages do not cause additional absorptions in the visible region compared with oxygen-ether linkages. It has been proven that PTEI films exhibit high refractive indices and low birefringence [15–17]. Thus, the present polymers might find some applications in advanced optical areas, such as high refractive index substrate for organic electroluminescent devices [18].

The solubility of the wholly-imidized PTEI films were evaluated in several typical solvents: organic polar aprotic solvent (NMP), inorganic strong acid (H_2SO_4), phenol solvent (*m*-cresol) and low polar solvent (2-methoxyethanol). The results are listed in table 1. It can be seen that all the PTEI films exhibit good resistance to phenol solvent and low polar solvent. The films kept their original shapes and the color of the solvent remained constant. All the films dissolved partially in H_2SO_4. Most of the films showed good durability in NMP in the tested time (24 h) except for PI-3. PI-3 has poor solvent resistance and the dissolution behavior of PI-3 in the tested solvents is different. For

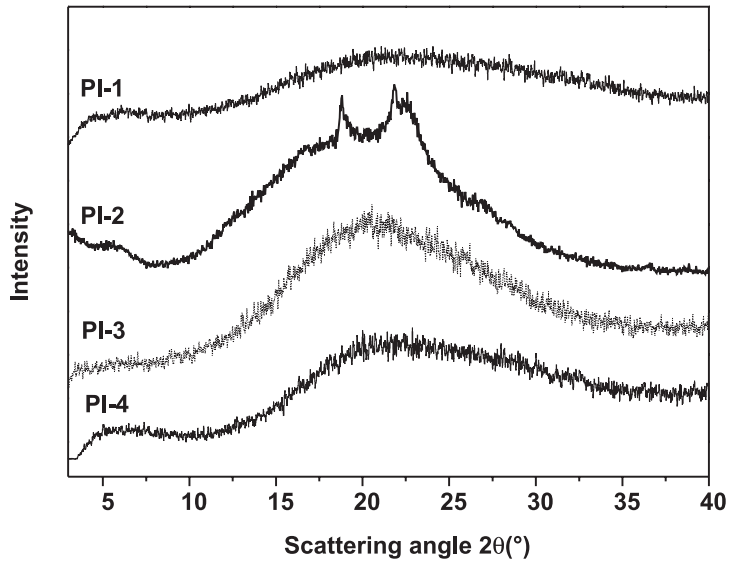

Figure 3. X-ray patterns of PTEI films.

example, PI-3 was completely dissolved in NMP during 3 h and the dissolution proceeded as swelling → softening → solving. In H_2SO_4, the film dissolved in 24 h and the course is darkening → cracking → solving. This might be due to the double functions of H_2SO_4, solvent and oxidizing agent.

3.3. Thermal properties

The thermal properties of the PTEIs were investigated by TGA, DSC and DMA measurements and the results are presented in table 2. It can be noticed that all the polymers exhibit good thermal stability up to 480°C both in nitrogen and in air. They also exhibited similar thermal decomposition behaviors either in nitrogen or in air. Very similar TGA curves have been recorded for all of the PTEIs, as shown in figure 5. For example, PI-3, derived from 3SDEA and 133APB, is expected to exhibit lower initial thermal decomposition temperatures (T_d) than those of the other analogues due to the more flexible *meta*-substituted molecular structures. However, they show similar T_d values.

It should also be noticed from Figure 6(b) that the present PTEIs show higher T_d values in air than those in nitrogen. For instance, the 5% weight loss temperatures ($T_{5\%}$) of the PTEIs in air range from 513.1–517.0°C, which are about 20°C higher than those in nitrogen. This phenomenon has also been reported on the other sulfur-containing polymers in the literature. Li and coworkers investigated the thermal decomposition of PPS film under different atmospheres using a high-resolution thermogravimetry analyzer [19].

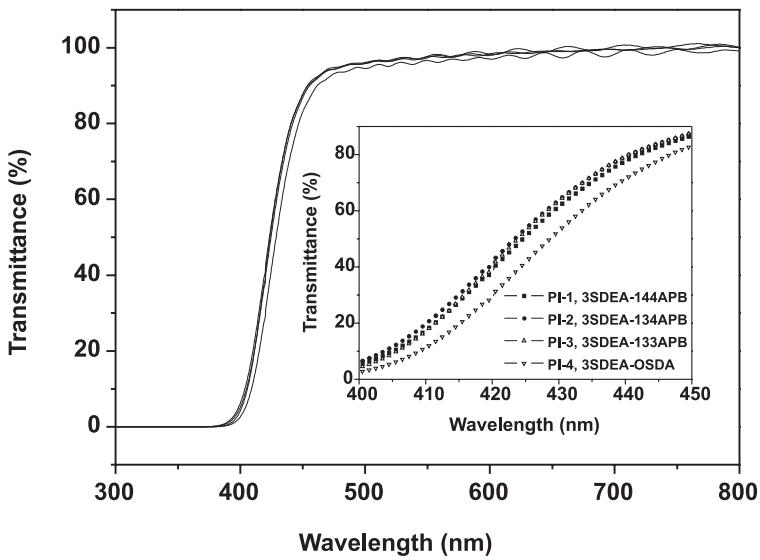

(a)

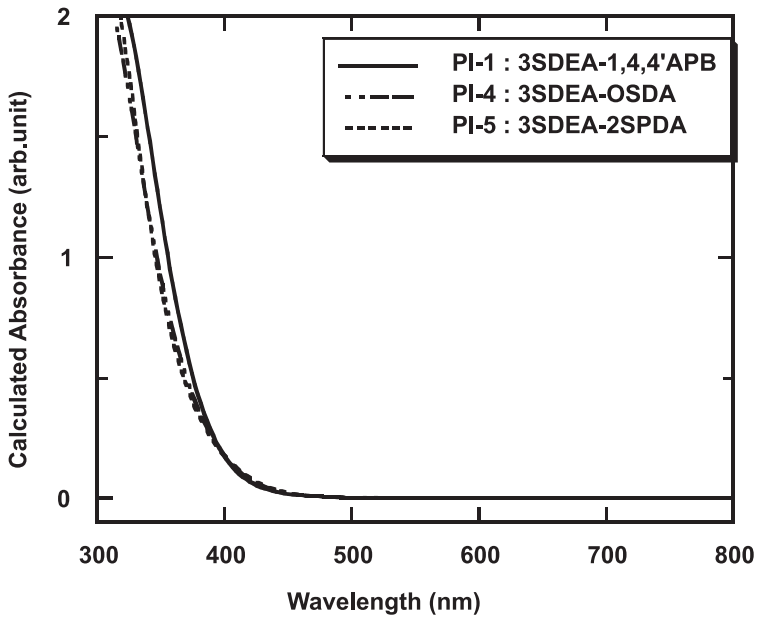

(b)

Figure 4. (a) Experimental and (b) calculated UV Vis absorption spectra of PTEI films (film thickness: $\sim$10 μm).

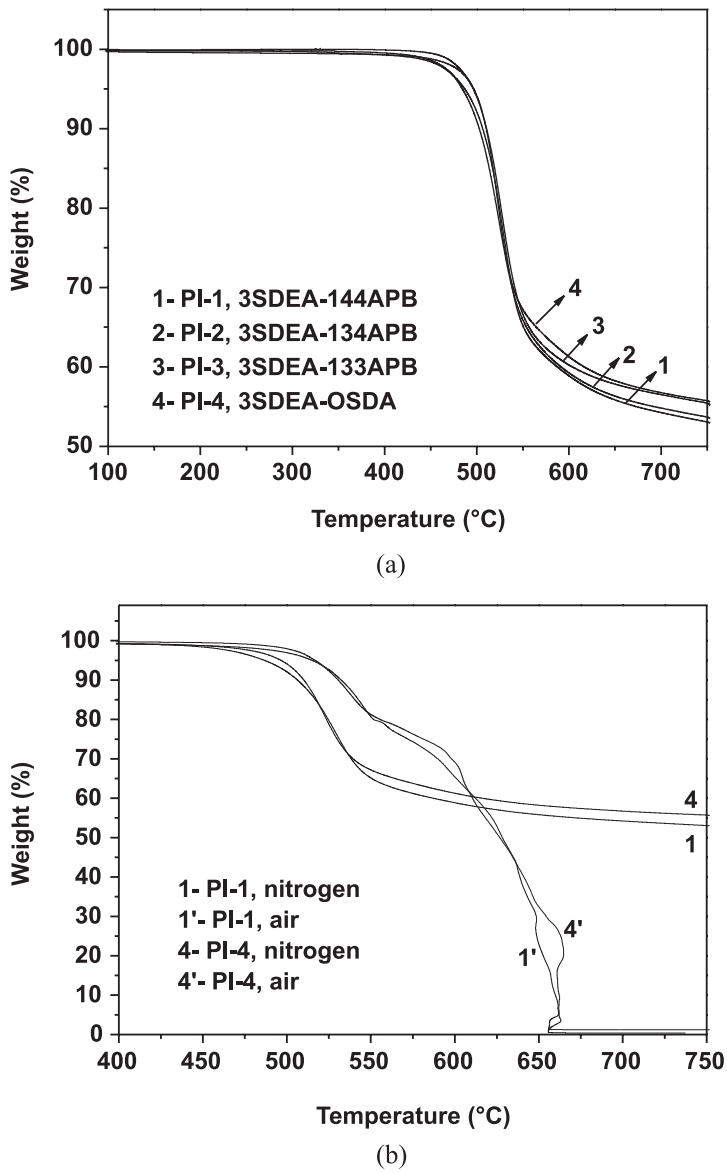

Figure 5. TGA curves of PTEIs: (a) in nitrogen; (b) comparison between in nitrogen and in air (10°C min^{-1}).

It was found that the T_d values of PPS increased in the following order: T_d (helium) $< T_d$ (nitrogren) $< T_d$ (argon) $< T_d$ (air). The author ascribed this phenomenon to the different thermal conductivities and densities of the gases. They also reported that the PPS

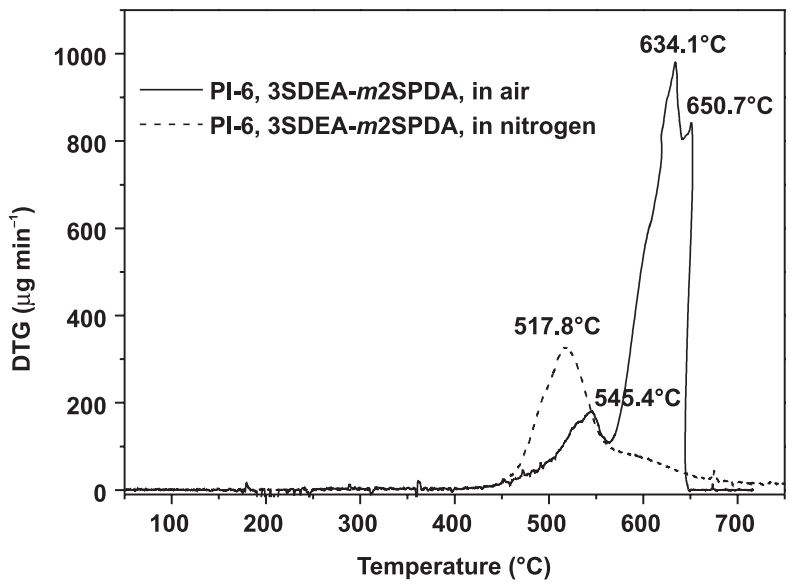

Figure 6. DTG curves for PI-6.

Table 2. Thermal properties of PTEI films[a].

PI	T_g (C)		T_m	$T_{5\%}$ (C)		$T_{10\%}$ (C)		R_{w750}
	DSC	DMA	(C)	air	N_2	air	N_2	(%)
PI-1	179.0	191.9	–[c]	515.2	486.9	532.4	506.4	53.1
PI-2	171.3	177.2	282.6	513.1	484.3	533.3	502.6	53.7
PI-3	154.8	153.1	–[c]	510.6	496.3	531.4	510.5	55.4
PI-4	189.5	191.5	–[c]	517.0	496.7	530.7	510.1	55.7
PI-5	191.2	–[b]	–[c]	497.2	491.1	514.8	504.4	56.8
PI-6	162.6	–[b]	329.1	514.7	486.0	535.9	501.6	56.4

[a] T_g: glass transition temperature; $T_{5\%}$, $T_{10\%}$: temperatures at 5% and 10% weight loss; T_m: melting point; R_{w750}: residual weight at 750°C in nitrogen.
[b] Not measured.
[c] Not detected.

showed a four-step degradation process in air. In the present research, similar thermal decomposition behaviors were observed for the PTEIs. As can be seen from the derivative thermogravimetry (DTG) curves of PI-6 illustrated in figure 6, the PTEIs show only one maximum decomposition stage in nitrogen (517.8°C) compared to three main decomposition stages in air (545.4°C, 634.1°C and 650.7°C). Kuroda and coworkers have reported that the major degradation mechanisms for aromatic thermoplastic polymers in

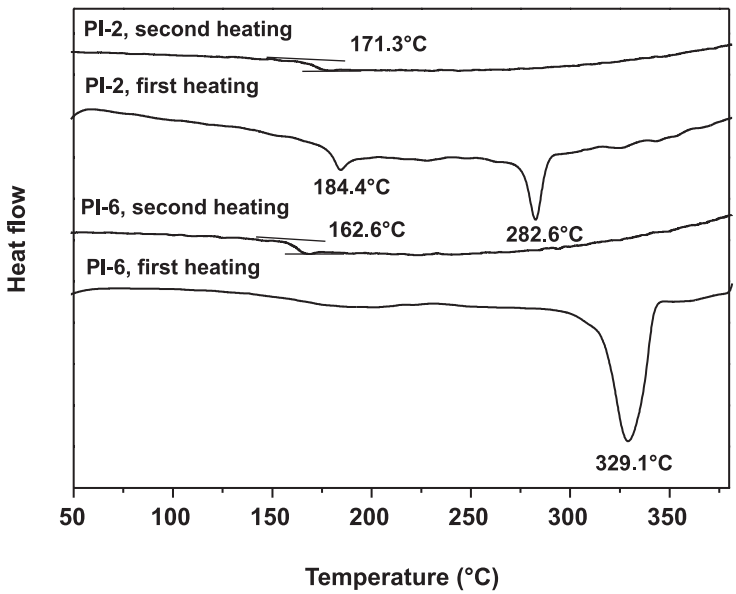

Figure 7. First and second heating for PI-2 and PI-6 (in nitrogen, 10°C min^{-1}).

the initial stage are crosslinking and chain scission according to GPC analysis [20]. It has been proven that for PEI, crosslinking is the dominant thermal degradation process [21]. Thus, the initial decomposition in air is mainly attributed to the intra- or inter-molecular crosslinking and the second and third are the degradation of aromatic moieties.

The PTEIs exhibit similar thermal decomposition behaviors. However, the glass transition temperatures are different, as can be authenticated by the DSC (figure 7) and DMA (figure 8) measurements. Generally, the present PTEIs show lower T_g values compared to the commercial PEIs, such as Aurum® (T_g: 250) [22], Ultem-1000® (T_g: 215°C) and Ultem-5000® (T_g: 235°C) [23]. The lower values of T_g are mainly attributed to the flexible thioether linkages in the molecular chains. Although the present PTEIs show T_g values of lower than 200°C, they might find applications in some special areas. For example, low-T_g (< 200°C) polyimides have been developed as adhesives for the protection of semiconductors [24] or superconducting wires [25, 26]. They exhibit excellent low temperature adhesion properties and radiation resistances.

The T_g values increase in the order of PI-3 < PI-6 < PI-2 < PI-1 < PI-4 < PI-5. Thus, the PTEIs with *para*-substituted structures (PI-1, PI-4 and PI-5) show higher T_g values than those of *meta*-substituted analogues (PI-2, PI-3 and PI-6). This trend is consistent with their structural linearity and rigidity, which has been clarified by Tamai et al. [27]. Among the latter, PI-3 with both of the *meta*-amino and *meta*-ether-substituted structures exhibits the lowest T_g. In the DMA curves, the T_g determined as the peak temperature

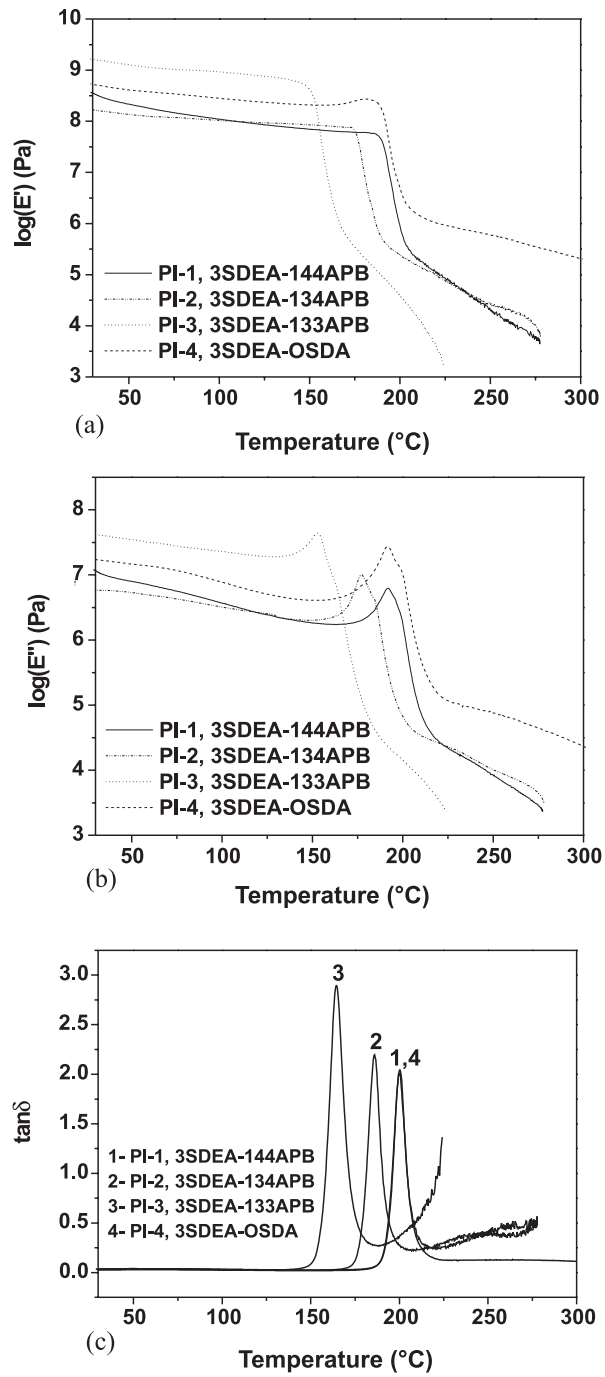

Figure 8. DMA curves of PI-1∼PI-4 (1 Hz, 2°C min^{-1}): (a) storage modulus E', (b) loss modulus E'' and (c) tan δ.

of loss modulus (E'') increase in the following order: PI-3 < PI-2 < PI-1 ≈ PI-4, which reveal a similar trend as demonstrated in the DSC measurement.

The crystallinity of the polyimides based on *meta*-substituted diamine (134APB) is well-known in the literature [28]. Ree et al. [29] reported that PMDA-3,4'-ODA [poly (pyromellitic-3,4'-oxydianiline)] PI exhibited a well-developed crystalline structure with highly-ordered molecular orientation and lateral packing based on an orthorhombic crystal unit cell, whereas PMDA-4,4'-ODA [poly(pyromellitic-4,4'-oxydianiline)] does not. These facts clearly indicate that *meta*-substituted diamines are more likely to afford fully extended polyimide chains with pseudo-rod like conformation than those of *para*-substituted diamines. In the present work, high crystallinity of PTEIs derived from 134APB (PI-2) and *m*2SPDA (PI-6) was also observed. For instance, clear melting points (282.8°C for PI-2 and 329.2°C for PI-6) were observed in the first DSC scan, as illustrated in figure 7. However the melting points disappeared in the second scan and only the glass transitions were recorded, probably due to the kinetically slow crystallization in the PTEIs from the melts.

4. CONCLUSIONS

A series of PTEIs have been prepared from a sulfur-containing dianhydride 3SDEA and various aromatic diamines. The effects of the structural varieties on the film properties, thermal properties, solvent resistances and optical transparency were discussed. The PTEI films are characterized by their good thermal and thermal-oxidative stabilities, good optical transparency in visible light region, good resistance to organic solvents and low T_g values. The high-sulfur-content PTEIs (PI-5 and PI-6) also have high refractive indices. In addition, preliminary experimental results show that the present PTEIs have good adhesion to metals such as aluminum. The good combined properties make them ideal candidates as low temperature adhesives and melt-processable laminates or films for high-tech fields.

NOTE

1. Author to whom correspondence should be addressed: e-mail: liujg@iccas.ac.cn.
2. Also at Department of Organic and Polymeric Materials, Tokyo Institute of Technology, 2-12-1-H120, O-okayama, Meguro-ku, Tokyo 152-8552, Japan

REFERENCES

[1] Hergenrother, P. M. (2003). The Use, Design, Synthesis, and Properties of High Performance/High Temperature Polymers: An Overview, *High Perform. Polym.,* **15**: 3–45.

[2] Watanabe, Y., Shibasaki, Y., Ando, S. and Ueda, M. (2005). Synthesis and characterization of polyimides with low dielectric constants from aromatic dianhydrides and aromatic diamine containing phenylene ether unit, *Polymer,* **46**: 5903–5908.

[3] Chen, B. K., Fang, Y. T. and Cheng, J. R. (2006). Synthesis of Low Dielectric Constant Polyetherimide Films, *Macromol. Symp.,* **242**: 34–39.

[4] Tanthapanichakoon, W., Hata, M., Nitta, K., Furuuchi, M., and Otani, Y. (2006). Mechanical degradation of filter polymer materials: Polyphenylene sulfide, *Polym. Degrad. Stab.,* **91:** 2614–2621.

[5] Tanglaw, R., Wilson, A. D., Hiroshi, N., Hideaki, K., Yoshihito, M. and Masanori, N. (2004). PPS-metal adhesion: a density functional theory-based study, *Solid State Commu.,* **132**: 405–408.

[6] Watanabe, Y., Shibasaki, Y., Ando, S. and Ueda, M. (2006). Synthesis and Characterization of Novel Low-*k* Polyimides from Aromatic Dianhydrides and Aromatic Diamine Containing Phenylene Ether and Perfluorobiphenyl Units, *Polym. J.,* **38**: 79–84.

[7] Mei, Z. and Chung, D. D. L. (2000). Effect of heating time below the melting temperature on polyphenylene sulfide adhesive joint development, *Inter. J. Adhe. & Adhe*., **20**: 273–277.

[8] Evans, T. L., Williams, F. J., Donahue, P. E. and Grade, M. M. (1984). Synthesis and polymerization of thioether dianhydride, *Polym. Prepr.,* **25**: 268–269.

[9] Glatz, F. P. and Mulhaupt, R. (1993). Syntheses and properties of soluble poly(arylene thioether imide)s and the corresponding poly(arylene sulfone imide)s, *Polym. Bull.,* **31**: 137–143.

[10] Mathias, L. J., Cei, G., Johnson, R. A. and Yoneyama, M. (1995). Poly(thioether imide)s via chloro-displacement polymerization, *Polym. Bull.,* **34**: 287-294.

[11] Ellison, M. M. and Taylor, L. T. (1997). Polyimide adhesives and aluminum, *J. Adhesion* **60**: 39–49.

[12] Liu, F., Wang, Z., Yang, H. L., Gao, L. X. and Ding, M. X. (2006). Synthesis of novel maleimide-terminated thioetherimide oligomer and its bulk copolymerization with reactive solvents, *Polymer,* **47**: 937–945.

[13] Glatz, F. P., Mulhaupt, R., Schultze, J. D. and Springer, J. (1994). Gas permeabilities and permselectivities of amorphous segmented 6F poly (arylene thioether imide)s and the corresponding poly(arylene sulfone imide)s, *J. Membr. Sci.,* **90**: 151–159.

[14] Terui, Y. and Ando, S. (2005). Refractive Indices and Thermo-Optic Coefficients of Aromatic Polyimides Containing Sulfur Atoms**,** *J. Photopolym. Sci. Tech.,* **18**: 337-340.

[15] Liu, J. G.., Nakamura, Y., Shibasaki, Y., Ando, S. and Ueda, M. (2007). Synthesis and Characterization of High Refractive Index Polyimides Derived from 4,4'-(*p*-Phenylenedisulfanyl)dianiline and Various Aromatic Tetracarboxylic Dianhydrides, *Polym. J.,* **39**: 543-550.

[16] Liu, J. G.., Nakamura, Y., Shibasaki, Y., Ando, S. and Ueda, M. (2007). Synthesis and Characterization of Highly Refractive Polyimides from 4,4'-Thiobis[(*p*-phenylenesulfanyl) aniline] and Various Aromatic Tetracarboxylic Dianhydrides, *J. Polym. Sci., Part A: Polym. Chem.,* in press.

[17] Liu, J. G.., Nakamura, Y., Shibasaki, Y., Ando, S. and Ueda, M. (2007). High Refractive Index Polyimides Derived from 2,7-Bis(4-aminophenylenesulfanyl)- thianthrene and Aromatic Dianhydrides, *Macromolecules,* **40**: 4614–4620.

[18] Nakamura, T., Fujii, H., Juni, N. and Tsutsumi, N. (2006). Enhanced Coupling of Light from Organic Electroluminescent Device Using Diffusive Particle Dispersed High Refractive Index Resin Substrate, *Opt. Rev.,* **13**: 104–110.

[19] Li, X. G., Huang, M. R., Bai, H. and Yang, Y. L. (2002). High-resolution thermogravimetry of polyphenylene sulfide film under four atmospheres, *J. Appl. Polym. Sci.,* **83**: 2053–2059.

[20] Kuroda, S., Terauchiro, K., Nagomi, K. and Mita, I. (1989). Degradation of aromatic polymers—I. Rates of crosslinking and chain scission during thermal degradation of several soluble aromatic polymers, *Europ. Polym. J.,* **25**: 1–7.

[21] Augh, L. and Gillespie, Jr. J. W. (2001). Degradation of Continuous Carbon Fiber Reinforced Polyetherimide Composites During Induction Heating**,** *J. Therm. Compos. Mater.,* **14**: 96–115.

[22] Tamai, S., Kuroki, T., Shibuya, A. and Yamaguchi, A. (2001). Synthesis and characterization of thermally stable semicrystalline polyimide based on 3,4'-oxydianiline and 3,3',4,4'-biphenyltetracarboxylic dianhydride, *Polymer,* **42**: 2373–2378.

[23] Sanchis, M. J., Diaz-Calleja, R., Jaimes, C., Belana, J., Canadas, J. C., Diego, J. A., Mudarra, M. and Sellares, J. (2004). A relaxational and conductive study on two poly(ether imide)s, *Polym. Int.,* **53**: 1368–1377.

[24] Tanabe, Y. and Matsuura, S. (2003). Adhesive film for semiconductor, lead frame having the adhesive film for semiconductor and semiconductor device, *Japanese Patent* 2003119440.

[25] Okamoto, K., Furuya, H., Nojiri, H. and Nagano, K. (1997). Wire material coating heat-fusion bonding laminated film, *Japanese Patent* 09109342.

[26] Tsuji, H., Kikuchi, T. and Furuya, H. (2002). Adhesive laminate film for coating accelerator beam tube, *Japanese Patent* 2002309218.

[27] Tamai, S., Yamaguchi, A. and Ohta, M. (1996). Melt processable polyimides and their chemical structures, *Polymer,* **37**: 3683–3692.

[28] Atsushi, M. (2006). High-Performance Design of Super-Engineering Plastics (Polyimides), *Kobunshi,* **55**: 874–977 (in Japanese).

[29] Ree, M., Nunes, T. L., Czornyj, G. and Volksen, W. (1992). Residual stress behavior of isomeric PMDA-ODA polyimides, *Polymer* **33**: 1228–1236.